Acta Cryst E CRYSTALLOGRAPHIC COMMUNICATIONS

ISSN 2056-9890

Bis[1,2-bis(4-fluorophenyl)ethylene-1,2-dithiolato(1−)]nickel(II)

Joseph B. Donahue,[a] Titir Das Gupta,[b] Laura Fiabane,[b] Xiaodong Zhang[b] and James P. Donahue[b]*

[a]Saint Paul's Catholic School, 917 South Jahncke Avenue, Covington, LA 70433, USA, and [b]Department of Chemistry, Tulane University, 6400 Freret Street, New Orleans, Louisiana 70118-5698, USA. *Correspondence e-mail: donahue@tulane.edu

Received 13 July 2025
Accepted 14 August 2025

Edited by J. Reibenspies, Texas A & M University, USA

Keywords: crystal structure; dithiolene; radical monoanion; nickel; electron-withdrawing; C—H→F hydrogen bonds.

CCDC reference: 2480642

Supporting information: this article has supporting information at journals.iucr.org/e

The crystal structure of the title compound, $[Ni(C_{14}H_8F_2S_2)_2]$ (**I**), reveals averaged S—C [1.708 (2) Å] and C—$C_{chelate}$ [1.395 (4) Å] bond lengths that are consistent with radical monoanionic ligands paired with a divalent Ni^{2+} ion. Molecules of **I** associate as dyads *via* intermolecular Ni···S close contacts of 3.396 (2) Å. This close association is enabled by a bending of both dithiolene ligands to the same side and away from the NiS_4 planar interior such that the angle between the seven atom mean planes defined by each NiS_2C_2 ring and the first C atom of each aryl substituent is 22.91 (8)°. These dyads form sheets in the *bc* plane that are held together in part by intermolecular C—H···F hydrogen bonds of 2.47 (4) Å.

1. Chemical context

Since the mid 1960s, when transition-metal dithiolene complexes first elicited interest because their electronic structure descriptions were at variance with classical formalisms (Eisenberg & Gray, 2011), applications arising from their optical, electrochemical, conducting and magnetic properties have continued to drive fundamental studies. Homoleptic nickel bis(dithiolene) complexes serve as reversibly bleachable dyes in laser Q-switching systems (Mueller-Westerhoff *et al.*, 1991) and as optical limiting absorbers (Tan *et al.*, 2000). Asymmetric Group 10 complexes with an ene-1,2-dithiolate donor and an α-dithione acceptor function as nonlinear optical materials with potential applications in optical switching devices, signal processing, *etc.* (Deplano *et al.*, 2010; Artizzu *et al.*, 2022). Partially oxidized Group 10 complexes with dmit [dmit = 2-thioxo-1,3-dithiole-4,5-dithiolate(2–)] support superconductivity in the crystalline state, a behavior that is rare for discrete coordination compounds (Cassoux, 1999; Faulmann & Cassoux, 2004; Kato, 2004). Dithiolene complexes sustain a variety of magnetic behaviors in the solid state (Robertson & Cronin, 2002; Faulmann & Cassoux, 2004), and they have more recently been investigated as a platform for molecule-based qubits (McGuire *et al.*, 2018, 2019). Dithiolene complexes of both nickel (Zarkadoulas *et al.*, 2016) and cobalt (McNamara *et al.*, 2012; Letko *et al.*, 2014) have been reported as highly active electrocatalysts for H_2-evolution. In this context, the structure of $K_2[Co(S_2C_2(C_6H_4\text{-}4\text{-}F)_2)_2]$ has been reported in 2014 (Letko *et al.*, 2014) and remains the only structurally authenticated coordination compound with this ligand variant. The corresponding charge-neutral nickel compound, although used earlier for the preparation of $[((F\text{-}4\text{-}C_6H_4)_2C_2S_2)_2W(CO)_2]$ (Sung & Holm, 2002) and used in a study of its formation of an

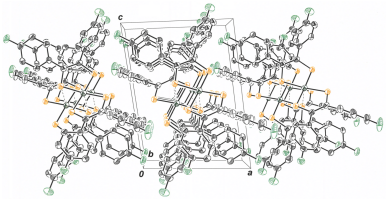

adduct with quadricyclane (Kajitani *et al.*, 1989), has not been characterized structurally. As part of an effort to fully map the range of reduction potentials observed for $[Ni(S_2C_2Ar_2)_2]$ (Ar = aryl substituent) compounds, we have obtained a crystalline sample of $[Ni(S_2C_2(C_6H_4\text{-}4\text{-}F)_2)_2]$ and subjected it to an X-ray diffraction study. We detail its structure herein, particularly in contrast to that of $[Ni(S_2C_2(C_6H_4\text{-}4\text{-}Cl)_2)_2]$.

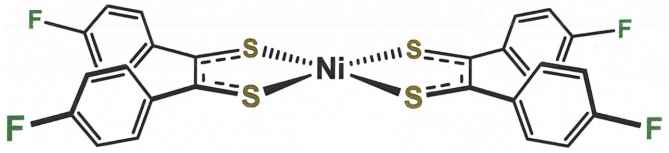

2. Structural commentary

An image of $[Ni(S_2C_2(C_6H_4\text{-}4\text{-}F)_2)_2]$, **I**, complete with atom labeling and 50% displacement ellipsoids, is presented in Fig. 1. The averaged S—C and C—$C_{chelate}$ bond lengths are 1.708 (2) and 1.395 (4) Å, respectively, values that are midway between the corresponding interatomic distances that have been experimentally established for the fully reduced ene-1,2-dithiolate form (Lim *et al.*, 2001) and the fully oxidized α-dithione redox state of the dithiolene ligand (Bigoli *et al.*, 2001). The dithiolene ligands in **I** are therefore in the half-reduced mono-anionic redox level (Lim *et al.*, 2001) that provides for charge neutrality when paired with a Ni^{2+} d^8 ion (Fig. 2).

The local geometry around Ni1 is square planar, but a moderate distortion is occasioned by a bending of the two dithiolene ligands to the same side of the central NiS_4 plane. The angle between the S1–S2–Ni1 and S3–S4–Ni1 planes is 11.62 (7)°, while the angle between the mean planes defined by each NiS_2C_2 chelate ring and the first carbon atom of each appended arene ring is double this magnitude at 22.92 (8)°. These differing values and a relatively modest 0.130 Å displacement of Ni1 from the S1–S2–S3–S4 mean plane emphasize that, while the molecule as a whole is bowl-shaped, its bottom is shallow, and the bent character is evident largely

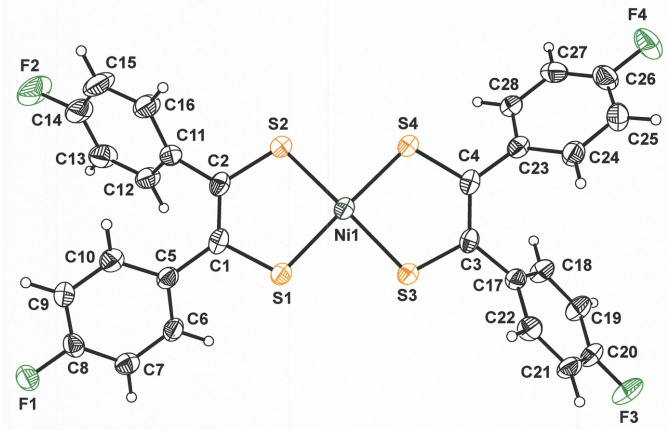

Figure 1
Displacement ellipsoid plot (50% probability) of $[Ni(S_2C_2(C_6H_4\text{-}4\text{-}F)_2)_2]$ with complete atom labeling.

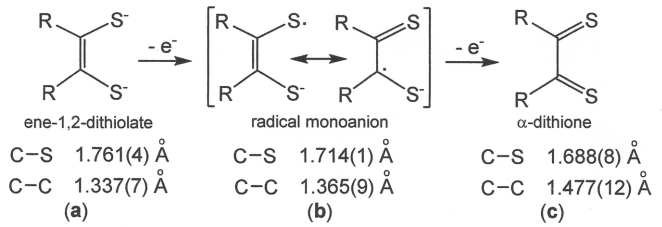

Figure 2
Redox levels of the dithiolene ligand with experimentally determined intraligand S—C and C—C bond lengths that are diagnostic of each redox state.

because of the peripheral organic groups. The angles formed between the pendant arene rings and the C_2S_2 fragment to which they are attached range from 42.7 (1) to 54.1 (1)° and average 47.63 (6)°.

The bent conformation displayed by **I** is a consequence of close intermolecular Ni···S contacts that place molecules into pairs with a face-to-face, but slightly offset, disposition on either side of an inversion center (Fig. 3). A rhomboidal shape is defined by this central Ni_2S_2 core. The intermolecular Ni1···S3 distance is 3.396 (2) Å, while the Ni1···Ni1 distance is 4.106 (1) Å. The former value is substantially less than the 3.8 Å sum of crystallographic radii for Ni (2.0 Å) and S (1.8 Å) (Batsanov, 2001), therefore implicating it as a decisive interaction in governing the crystalline packing arrangement. This interaction is reinforced by a 2.86 (5) Å close contact between S2 of one molecule and H22 of its centrosymmetric counterpart (Fig. 3). A mononuclear species is pertinent to the solution phase, however, as the ^{19}F, ^{13}C, and ^{1}H NMR spectra show the simpler sets of signals anticipated for a D_{2h}-symmetric structure *vs* one with only C_i symmetry.

3. Supramolecular features

The outward bowing of the dithiolene ligands that enables close approach of the NiS_4 interior of two molecules provides a concave appearance to the dyadic assembly. These dyads are related by simple translation along the *b* axis of the unit cell (Fig. 4) such that they eclipse one another in stacks when

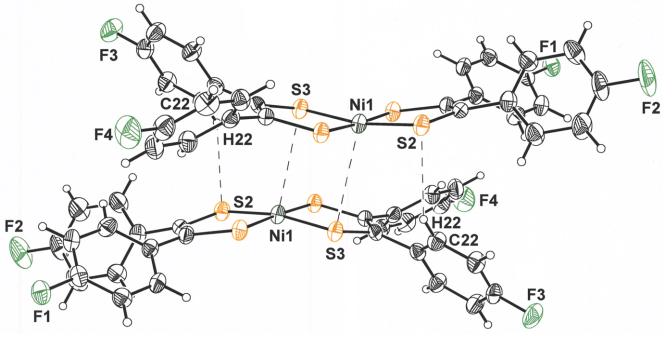

Figure 3
Displacement ellipsoid plot (50% probability) of $[Ni(S_2C_2(C_6H_4\text{-}4\text{-}F)_2)_2]$ showing its close interaction with a neighboring molecule across an inversion center.

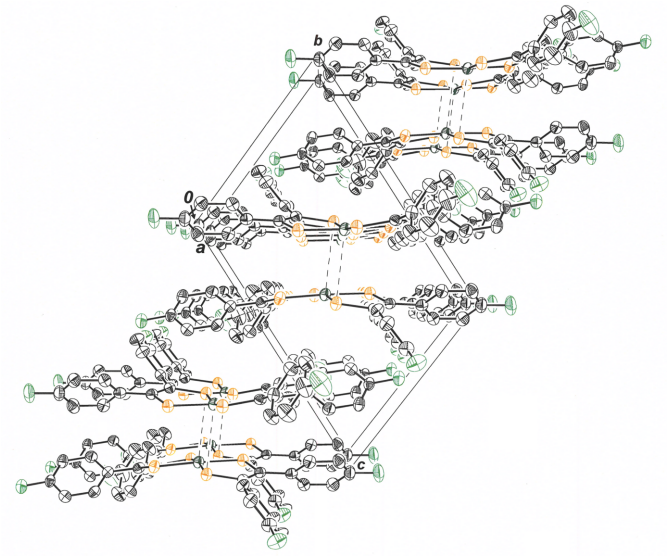

Figure 4
View down the *a* axis of the cell illustrating how the dyads shown in Fig. 2 are related by translation along the *b* axis. Displacement ellipsoids are shown at 50% probability, and all H atoms are omitted for clarity.

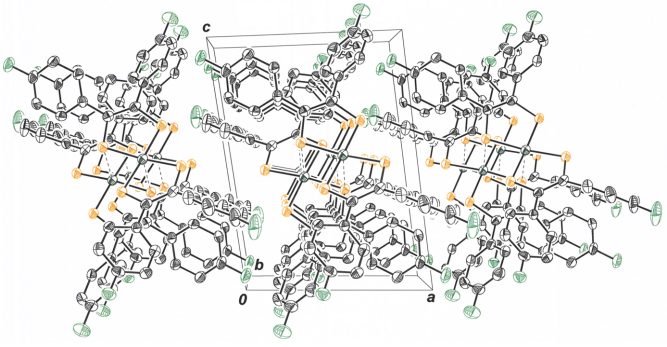

Figure 5
View down the *b* axis of the cell illustrating how the dyads shown in Fig. 2 form stacks in this axis direction. Displacement ellipsoids are shown at 50% probability, and all H atoms are omitted for clarity.

Table 1
Hydrogen-bond geometry (Å, °).

D—H···*A*	*D*—H	H···*A*	*D*···*A*	*D*—H···*A*
C19—H19···F1^{i}	1.00 (4)	2.47 (4)	3.136 (5)	123 (3)

Symmetry code: (i) $x, y+1, z+1$.

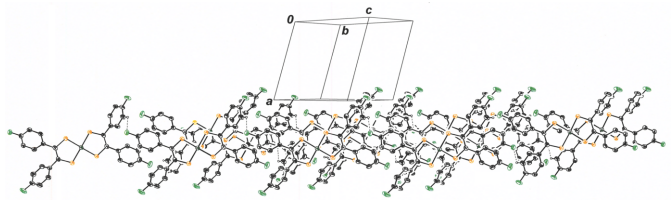

Figure 7
View along the *bc* plane of the packing for **I**, emphasizing the sheet-like arrangement of molecules in this direction. Displacement ellipsoids are shown at the 50% level, and all H atoms are omitted for clarity.

viewed down the *b* axis (Fig. 5). Within the *bc* plane, each dyad is held in place by an array of four C—H···F hydrogen bonds (Table 1), with F1 from each molecule in the pair acting as acceptor and C19—H19 from the other ligand of each molecule serving as donor (Fig. 6). The H19···F1 and C19···F1 interatomic distances are 2.47 (4) Å and 3.136 (5) Å, respectively. The perspective in Fig. 7 is approximately orthogonal to that in Fig. 6 and emphasizes the sheet-like arrangement of molecules within the *bc* plane.

4. Database survey

The arrangement for **I** has qualitative similarity to the fashion in which molecules of [Ni(S_2C_2(C_6H_4-4-Cl)$_2$)$_2$] (**II**) are juxtaposed in the crystalline state [Fig. 8(*b*)] (Koehne *et al.*, 2022). Pairs of **II** are also disposed around an inversion center in $P\overline{1}$, but the degree of bending of the aryl substituents away from one another is somewhat less than in **I**. The angle between the seven atom mean planes defined by the NiS_2C_2 chelate rings and the first carbon atom of the arene rings is 11.87 (5)°,

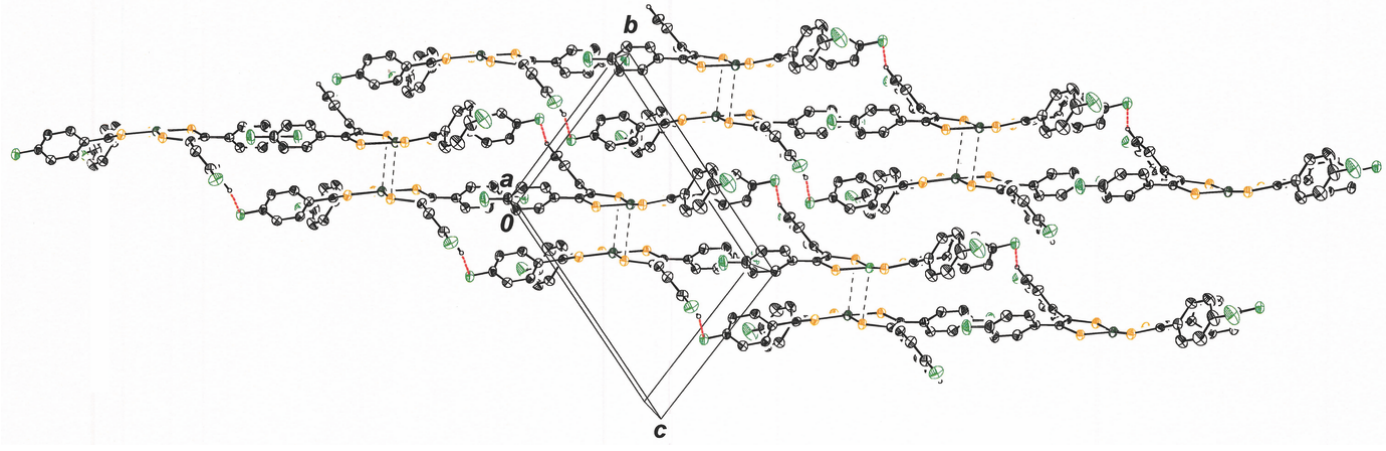

Figure 6
View down the *a* axis of the cell illustrating how the dyads of **I** interact in the *bc* plane *via* F···C—H hydrogen bonds. All H atoms are omitted except those involved in the F···C—H hydrogen bonding. The symmetry operation relating molecules that are participants in a F···C—H hydrogen bond is *x*, *y* + 1, *z* + 1. Displacement ellipsoids are presented at the 50% probability level.

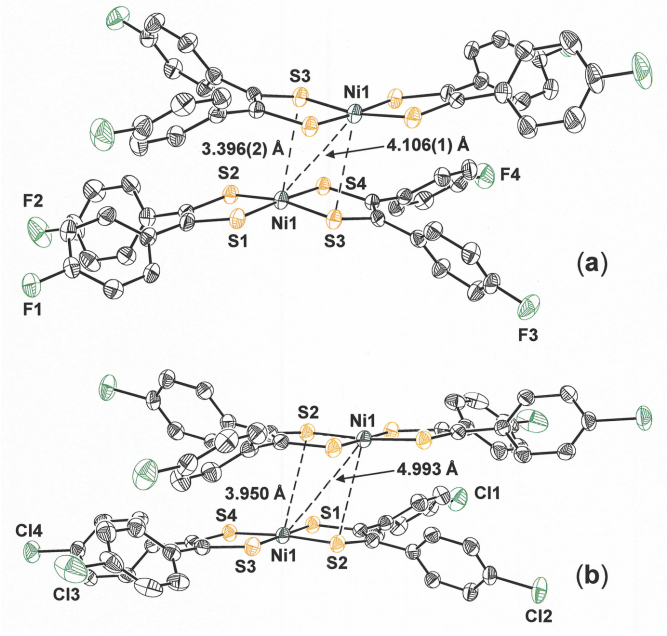

Figure 8
Contrast between the dyadic pairs of $[Ni(S_2C_2(C_6H_4\text{-}4\text{-}F)_2)_2]$ (**a**) *vs.* $[Ni(S_2C_2(C_6H_4\text{-}4\text{-}Cl)_2)_2]$ (**b**). Closer association of molecules in (**a**) than (**b**) is enabled by greater bending of the dithiolene ligands away from one another. Displacement ellipsoids are shown at 50% probability, and all H atoms are omitted for clarity.

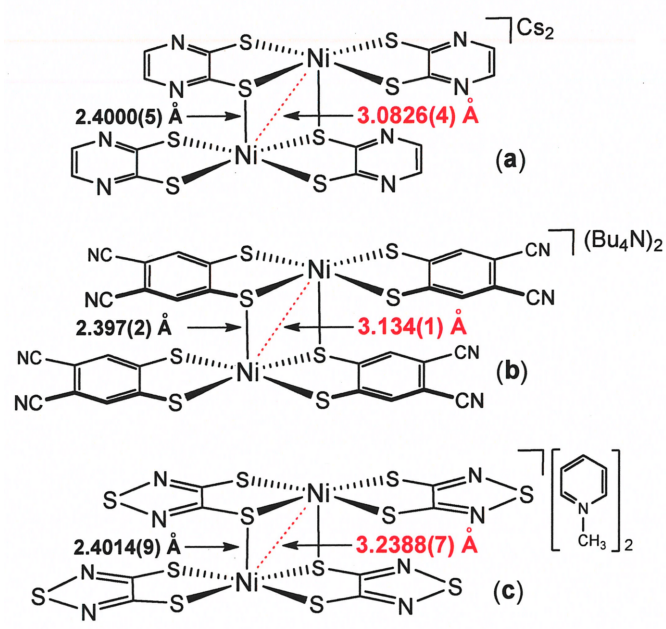

Figure 9
Known dimeric Ni bis(dithiolene) complexes shown with intermolecular Ni···S and Ni···Ni distances.

approximately half the magnitude of the same distortion in **I**. Because the steric crowding between its Cl-4-C_6H_4 substituents is less alleviated by bending away from one another, molecules of **II** associate less closely, with a Ni···Ni distance of 4.933 Å and an intermolecular Ni···S distance of 3.950 Å (Fig. 8). This contrast between **I** and **II** may reflect an attenuated basicity to the dithiolene sulfur atoms in **I**, owing to the greater electron-withdrawing power of F over Cl, such that the Lewis acid character of its Ni^{2+} ion is only fully alleviated by the additional interaction with a sulfur lone pair from a neighboring molecule.

Other crystallographically characterized nickel bis(dithiolene) complexes that are symmetrically substituted with aryl groups include $[Ni(S_2C_2Ph_2)_2]$ (Megnamisi-Belombe & Nuber, 1989; Kuramoto & Asao, 1990), $[Ni(S_2C_2(C_6H_4\text{-}4\text{-}CH_3)_2)_2]$ (Miao *et al.*, 2011), $[Ni(S_2C_2(C_6H_4\text{-}4\text{-}OCH_3)_2)_2]$ (Arumugam *et al.*, 2007), $[Ni(S_2C_2(C_6H_4\text{-}4\text{-}^t Bu)_2)_2]$ (Das Gupta *et al.*, 2023), and $[Ni(S_2C_2(C_6H_3\text{-}3,5\text{-}(CH_3)_2)_2]$ (Das Gupta *et al.*, 2025). In these cases, such other intermolecular interactions as aryl C—H···π_{arene}, CH_3···π_{arene}, or aryl C—H···π NiS_2C_2 hydrogen bonds form the basis for packing in the crystalline state rather than Ni···S close contacts as in **I**.

Although charge neutral diaryl-substituted nickel bis(dithiolene) complexes other than **I** and **II** do not appear to form paired interactions in the crystalline state, anionic nickel complexes with the related pyrazine-2,3-dithiolate (pyzdt) form either stacked monomers or dimers, depending upon the particular identity of the counter-cation (Takaishi *et al.*, 2013). With Cs^+, dimeric $[[Ni(pyzdt)_2]_2]^{2-}$ prevails with an Ni···Ni separation of 3.0826 (4) Å and an intermolecular Ni···S distance of 2.4000 (5) Å (Fig. 9). Similarly, nickel complexes with 4,5-dicyanobenzene-1,2-dithiolate (dcbdt) (Simão *et al.*, 2001) and 1,2,5-thiadiazole-3,4-dithiolate (tdas) (Chen *et al.*, 2016) form dianionic dimers with bridging Ni···S and interatomic distances that are the same as in $[[Ni(pyzdt)_2]_2]^{2-}$ within experimental error {Ni···S: 2.397 (2) Å in $[[Ni(dcbdt)_2]_2]^{2-}$, 2.4014 (9) Å in $[[Ni(tdas)_2]_2]^{2-}$}. However, the Ni···Ni separations vary substantially from that in $[[Ni(pyzdt)_2]_2]^{2-}$ {3.134 (1) Å in $[[Ni(dcbdt)_2]_2]^{2-}$ and 3.2388 (7) Å in $[[Ni(tdas)_2]_2]^{2-}$} because the Ni···S distances within the mononuclear fragments of these several complexes differ somewhat. In all these instances, the strong dimeric interaction is driven by antiferromagnetic coupling of the radical monoanionic fragments (Fig. 2) rather than by presumed Lewis acid–base pairing as in **I**.

5. Synthesis and crystallization

The procedure followed was a modification of that described by Mayweg & Schrauzer (1965). An oven-dried 100 mL Schlenk flask was charged with P_4S_{10} (3.502 g, 7.88 mmol), 1,2-bis(4-fluorophenyl)ethane-1,2-dione (2.010 g, 8.16 mmol), and 20 mL of dry dioxane. This mixture was placed under an N_2 atmosphere with a series of rapid evacuations and backfills and then was vigorously refluxed for 3 h. After cooling to ambient temperature, the heterogeneous mixture was filtered under N_2 *via* filter cannula to afford an amber-colored filtrate. A solution of $[Ni(OH_2)_6]Cl_2$ (1.001 g, 4.21 mmol) in degassed, deionized H_2O (20 mL) was transferred to this filtrate, and the mixture was again refluxed with stirring for 3 h. The dark reaction mixture was slowly cooled to ambient temperature overnight. The dark precipitate that formed was collected by vacuum filtration on a Hirsch funnel and washed with portions

Table 2
Experimental details.

Crystal data	
Chemical formula	$[Ni(C_{14}H_8F_2S_2)_2]$
M_r	615.36
Crystal system, space group	Triclinic, $P\overline{1}$
Temperature (K)	150
a, b, c (Å)	9.995 (2), 10.386 (2), 13.958 (3)
α, β, γ (°)	109.61 (3), 90.51 (3), 107.27 (3)
V (Å^3)	1293.7 (5)
Z	2
Radiation type	Mo $K\alpha$, λ = 0.71073 Å
μ (mm^{-1})	1.12
Crystal size (mm)	0.09 × 0.07 × 0.03
Data collection	
Diffractometer	Bruker D8
Absorption correction	Multi-scan (*SADABS*; Krause *et al.*, 2015)
T_{min}, T_{max}	0.823, 0.970
No. of measured, independent and observed [$I > 2\sigma(I)$] reflections	31779, 4774, 3330
R_{int}	0.079
Refinement	
$R[F^2 > 2\sigma(F^2)]$, $wR(F^2)$, S	0.044, 0.110, 1.05
No. of reflections	4774
No. of parameters	398
H-atom treatment	All H-atom parameters refined
$\Delta\rho_{max}$, $\Delta\rho_{min}$ (e Å^{-3})	0.60, −0.55

Computer programs: *APEX5* and *SAINT* (Bruker, 2024), *SHELXT2018/2* (Sheldrick, 2015*a*), *SHELXL2019/2* (Sheldrick, 2015*b*) and *SHELXTL* (Sheldrick, 2008).

of H_2O (2 × 10 mL), MeOH (2 × 10 mL), and Et_2O (2 × 10 mL). After drying overnight, **I** was obtained in the form of a dark powder. Yield: 0.684 g, 1.11 mmol, 27.2%. R_f = 0.73 in 1:1 CH_2Cl_2:hexane. ^{1}H NMR (δ, ppm in $CDCl_3$): 7.35 (*ddt*, J = 8.4, 5.3, 2.5 Hz, 8H), 7.04–6.97 (*m*, 8H). ^{13}C NMR (δ, ppm in $CDCl_3$): 180.4 (*s*), 163.3 (*d*, J_{FC} = 251 Hz), 137.3 (*d*, J = 3.5 Hz), 130.9 (*d*, J = 8.4 Hz), 115.9 (*d*, J = 21.8 Hz). ^{19}F NMR (δ, ppm in $CDCl_3$): (+50.66 relative to C_6F_6 internal standard). UV-vis [CH_2Cl_2, λ_{max} nm (ε_M, $M^{-1}\cdot cm^{-1}$)]: 270 (15,000), 315 (19,100), 600 (90), 860 (12,400). MS (MALDI$^+$) Calculated for $[C_{28}H_{16}F_4S_4Ni]^+$: *m*/*z* 613.94196; Observed: *m*/*z* 613.842; Error (δ): 163 ppm. Cyclic voltammetry (CH_2Cl_2, [^{n}Bu$_4$N][PF$_6$] supporting electrolyte, Cp_2Fe^+/Cp_2Fe as reference): $\mathbf{I} + e^- \rightarrow [\mathbf{I}]^-$, −0.40 V; $[\mathbf{I}]^- + e^- \rightarrow [\mathbf{I}]^{2-}$, −1.22 V.

6. Refinement

Hydrogen atoms were added in calculated positions and refined with isotropic displacement parameters that were 1.2 times those of the carbon atoms to which they were attached. The C—H distance assumed was 0.95 Å. Crystal data, data collection and structure refinement details are summarized in Table 2.

Funding information

Funding for this research was provided by: National Science Foundation, Directorate for Mathematical and Physical Sciences (grant No. 1836589 to James P. Donahue; award No. 1228232).

References

Artizzu, F., Espa, D., Marchiò, L., Pilia, L., Serpe, A. & Deplano, P. (2022). *Inorg. Chim. Acta* **531**, 120731.
Arumugam, K., Bollinger, J. E., Fink, M. & Donahue, J. P. (2007). *Inorg. Chem.* **46**, 3283–3288.
Batsanov, S. S. (2001). *Inorg. Mater.* **37**, 871–885.
Bigoli, F., Chen, C.-T., Wu, W.-C., Deplano, P., Mercuri, M. L., Pellinghelli, M. A., Pilia, L., Pintus, G., Serpe, A. & Trogu, E. F. (2001). *Chem. Commun.* pp. 2246–2247.
Bruker (2024). *APEX5* and *SAINT*. Bruker AXS Inc., Madison, Wisconsin, USA.
Cassoux, P. (1999). *Coord. Chem. Rev.* **185–186**, 213–232.
Chen, X.-X., Qiao, F., Wang, C.-F., Chi, Y.-H., Cottrill, E., Pan, N., Shi, J.-M., Zhu-Ge, W.-W., Fu, Y.-X., Xu, J. & Qian, X.-P. (2016). *J. Mol. Struct.* **1107**, 157–161.
Das Gupta, T., Applebaum, J., Broussard, W., Mack, C., Wu, C., Mague, J. T. & Donahue, J. P. (2023). *Acta Cryst.* E**79**, 182–186.
Das Gupta, T., Guite, J., Hirt, L. W., Zhang, X. & Donahue, J. P. (2025). *Acta Cryst.* E**81**, 534–537.
Deplano, P., Pilia, L., Espa, D., Mercuri, M. L. & Serpe, A. (2010). *Coord. Chem. Rev.* **254**, 1434–1447.
Eisenberg, R. & Gray, H. B. (2011). *Inorg. Chem.* **50**, 9741–9751.
Faulmann, C. & Cassoux, P. (2004). *Prog. Inorg. Chem.* **52**, 399–489.
Kajitani, M., Kohara, M., Kitayama, T., Akiyama, T. & Sugimori, A. (1989). *J. Phys. Org. Chem.* **2**, 131–145.
Kato, R. (2004). *Chem. Rev.* **104**, 5319–5346.
Koehne, S., Mirmelli, B., Mague, J. T. & Donahue, J. P. (2022). *IUCrData* **7**, x220148.
Krause, L., Herbst-Irmer, R., Sheldrick, G. M. & Stalke, D. (2015). *J. Appl. Cryst.* **48**, 3–10.
Kuramoto, N. & Asao, K. (1990). *Dyes Pigments* **12**, 65–76.
Letko, C. S., Panetier, J. A., Head-Gordon, M. & Tilley, T. D. (2014). *J. Am. Chem. Soc.* **136**, 9364–9376.
Lim, B. S., Fomitchev, D. V. & Holm, R. H. (2001). *Inorg. Chem.* **40**, 4257–4262.
McGuire, J., Miras, H. N., Donahue, J. P., Richards, E. & Sproules, S. (2018). *Chem. A Eur. J.* **24**, 17598–17605.
McGuire, J., Miras, H. N., Richards, E. & Sproules, S. (2019). *Chem. Sci.* **10**, 1483–1491.
McNamara, W. R., Han, Z., Yin, C.-J., Brennessel, W. W., Holland, P. L. & Eisenberg, R. (2012). *Proc. Natl Acad. Sci. USA* **109**, 15594–15599.
Megnamisi-Belombe, M. & Nuber, B. (1989). *Bull. Chem. Soc. Jpn* **62**, 4092–4094.
Miao, Q., Gao, J., Wang, Z., Yu, H., Luo, Y. & Ma, T. (2011). *Inorg. Chim. Acta* **376**, 619–627.
Mueller-Westerhoff, U. T., Vance, B. & Ihl Yoon, D. (1991). *Tetrahedron* **47**, 909–932.
Robertson, N. & Cronin, L. (2002). *Coord. Chem. Rev.* **227**, 93–127.
Schrauzer, G. N. & Mayweg, V. P. (1965). *J. Am. Chem. Soc.* **87**, 1483–1489.
Sheldrick, G. M. (2008). *Acta Cryst.* A**64**, 112–122.
Sheldrick, G. M. (2015*a*). *Acta Cryst.* A**71**, 3–8.
Sheldrick, G. M. (2015*b*). *Acta Cryst.* C**71**, 3–8.
Simão, D., Alves, H., Belo, D., Rabaça, S., Lopes, E. B., Santos, I. C., Gama, V., Duarte, M. T., Henriques, R. T., Novais, H. & Almeida, M. (2001). *Eur. J. Inorg. Chem.* pp. 3119–3126.
Sung, K.-M. & Holm, R. H. (2002). *J. Am. Chem. Soc.* **124**, 4312–4320.
Takaishi, S., Hada, M., Ishihara, N., Breedlove, B. K., Katoh, K. & Yamashita, M. (2013). *Polyhedron* **52**, 333–338.
Tan, W. L., Ji, W., Zuo, J. L., Bai, J. F., You, X. Z., Lim, J. H., Yang, S., Hagan, D. J. & Van Stryland, E. W. (2000). *Appl. Phys. B* **70**, 809–812.
Zarkadoulas, A., Field, M. J., Papatriantafyllopoulou, C., Fize, J., Artero, V. & Mitsopoulou, C. A. (2016). *Inorg. Chem.* **55**, 432–444.

supporting information

Acta Cryst. (2025). E**81**, 874-878 [https://doi.org/10.1107/S2056989025007303]

Bis[1,2-bis(4-fluorophenyl)ethylene-1,2-dithiolato(1−)]nickel(II)

Joseph B. Donahue, Titir Das Gupta, Laura Fiabane, Xiaodong Zhang and James P. Donahue

Computing details

Bis[1,2-bis(4-fluorophenyl)ethylene-1,2-dithiolato(1-)]nickel(II)

Crystal data

$[Ni(C_{14}H_8F_2S_2)_2]$
$M_r = 615.36$
Triclinic, $P\overline{1}$
$a = 9.995$ (2) Å
$b = 10.386$ (2) Å
$c = 13.958$ (3) Å
$\alpha = 109.61$ (3)°
$\beta = 90.51$ (3)°
$\gamma = 107.27$ (3)°
$V = 1293.7$ (5) Å^3
$Z = 2$
$F(000) = 624$
$D_x = 1.580$ Mg m^{-3}
Mo $K\alpha$ radiation, $\lambda = 0.71073$ Å
Cell parameters from 6123 reflections
$\theta = 2.2$–24.3°
$\mu = 1.12$ mm^{-1}
$T = 150$ K
Prism, black
0.09 × 0.07 × 0.03 mm

Data collection

Bruker D8 diffractometer
Radiation source: sealed tube
Flat graphite monochromator
Detector resolution: 7.391 pixels mm^{-1}
ω and φ scans
Absorption correction: multi-scan (*SADABS*; Krause *et al.*, 2015)
$T_{min} = 0.823$, $T_{max} = 0.970$
31779 measured reflections
4774 independent reflections
3330 reflections with $I > 2\sigma(I)$
$R_{int} = 0.079$
$\theta_{max} = 25.5°$, $\theta_{min} = 2.5°$
$h = -12\rightarrow12$
$k = -12\rightarrow12$
$l = -16\rightarrow16$

Refinement

Refinement on F^2
Least-squares matrix: full
$R[F^2 > 2\sigma(F^2)] = 0.044$
$wR(F^2) = 0.110$
$S = 1.05$
4774 reflections
398 parameters
0 restraints
Primary atom site location: Intrinsic Phasing
Secondary atom site location: difference Fourier map
Hydrogen site location: difference Fourier map
All H-atom parameters refined
$w = 1/[\sigma^2(F_o^2) + (0.0455P)^2 + 0.6394P]$ where $P = (F_o^2 + 2F_c^2)/3$
$(\Delta/\sigma)_{max} = 0.001$
$\Delta\rho_{max} = 0.60$ e Å^{-3}
$\Delta\rho_{min} = -0.55$ e Å^{-3}

Special details

Geometry. All esds (except the esd in the dihedral angle between two l.s. planes) are estimated using the full covariance matrix. The cell esds are taken into account individually in the estimation of esds in distances, angles and torsion angles; correlations between esds in cell parameters are only used when they are defined by crystal symmetry. An approximate (isotropic) treatment of cell esds is used for estimating esds involving l.s. planes.

Fractional atomic coordinates and isotropic or equivalent isotropic displacement parameters (Å²)

	x	*y*	*z*	U_{iso}*/U_{eq}
Ni1	0.60045 (5)	1.37615 (5)	0.54003 (3)	0.02848 (15)
S1	0.48356 (9)	1.18073 (10)	0.42242 (7)	0.0296 (2)
S2	0.79331 (9)	1.32928 (10)	0.51093 (7)	0.0309 (2)
S3	0.40505 (9)	1.39858 (10)	0.58778 (7)	0.0296 (2)
S4	0.71238 (9)	1.56654 (10)	0.66330 (7)	0.0292 (2)
F1	0.3963 (2)	0.5400 (2)	0.08030 (15)	0.0381 (5)
F2	1.1261 (3)	0.8567 (3)	0.2995 (3)	0.0803 (10)
F3	−0.0292 (2)	1.5603 (3)	0.90721 (18)	0.0509 (6)
F4	0.8195 (3)	2.1168 (3)	1.08009 (18)	0.0620 (7)
C1	0.6030 (4)	1.0919 (4)	0.3789 (3)	0.0295 (8)
C2	0.7435 (4)	1.1591 (4)	0.4219 (3)	0.0277 (8)
C3	0.4465 (4)	1.5376 (4)	0.7026 (3)	0.0272 (8)
C4	0.5882 (4)	1.6177 (4)	0.7369 (3)	0.0286 (8)
C5	0.5479 (4)	0.9474 (4)	0.2984 (3)	0.0276 (8)
C6	0.4212 (4)	0.8507 (4)	0.3048 (3)	0.0300 (9)
H6	0.373 (3)	0.883 (3)	0.365 (3)	0.026 (9)*
C7	0.3680 (4)	0.7146 (4)	0.2306 (3)	0.0322 (9)
H7	0.282 (4)	0.653 (4)	0.235 (3)	0.031 (10)*
C8	0.4452 (4)	0.6772 (4)	0.1513 (3)	0.0305 (9)
C9	0.5695 (4)	0.7698 (4)	0.1405 (3)	0.0348 (9)
H9	0.622 (4)	0.748 (4)	0.089 (3)	0.041 (11)*
C10	0.6201 (4)	0.9057 (4)	0.2136 (3)	0.0343 (9)
H10	0.705 (4)	0.971 (4)	0.207 (2)	0.025 (9)*
C11	0.8517 (4)	1.0849 (4)	0.3954 (3)	0.0308 (9)
C12	0.8265 (4)	0.9498 (4)	0.4025 (3)	0.0348 (9)
H12	0.749 (4)	0.908 (4)	0.427 (2)	0.021 (9)*
C13	0.9186 (4)	0.8727 (5)	0.3712 (4)	0.0453 (11)
H13	0.902 (4)	0.788 (4)	0.375 (3)	0.032 (11)*
C14	1.0366 (4)	0.9341 (5)	0.3328 (4)	0.0509 (12)
C15	1.0676 (4)	1.0671 (5)	0.3276 (4)	0.0555 (13)
H15	1.146 (4)	1.104 (4)	0.304 (3)	0.042 (11)*
C16	0.9753 (4)	1.1448 (5)	0.3597 (3)	0.0419 (10)
H16	0.988 (4)	1.229 (4)	0.348 (3)	0.038 (11)*
C17	0.3250 (3)	1.5554 (4)	0.7605 (3)	0.0276 (8)
C18	0.3276 (4)	1.5697 (4)	0.8632 (3)	0.0343 (9)
H18	0.408 (4)	1.568 (3)	0.895 (2)	0.023 (9)*
C19	0.2092 (4)	1.5709 (5)	0.9130 (3)	0.0375 (10)
H19	0.206 (4)	1.572 (4)	0.985 (3)	0.035 (10)*
C20	0.0879 (4)	1.5595 (4)	0.8582 (3)	0.0354 (9)

C21	0.0799 (4)	1.5467 (4)	0.7578 (3)	0.0337 (9)
H21	−0.001 (4)	1.543 (4)	0.721 (3)	0.032 (10)*
C22	0.1993 (4)	1.5444 (4)	0.7088 (3)	0.0319 (9)
H22	0.189 (4)	1.530 (4)	0.635 (3)	0.039 (10)*
C23	0.6438 (4)	1.7467 (4)	0.8297 (3)	0.0289 (8)
C24	0.5873 (4)	1.8608 (4)	0.8526 (3)	0.0339 (9)
H24	0.511 (5)	1.849 (5)	0.807 (3)	0.061 (14)*
C25	0.6477 (4)	1.9861 (5)	0.9361 (3)	0.0422 (10)
H25	0.612 (4)	2.061 (4)	0.945 (3)	0.042 (11)*
C26	0.7612 (4)	1.9942 (4)	0.9964 (3)	0.0426 (10)
C27	0.8180 (4)	1.8858 (5)	0.9774 (3)	0.0392 (10)
H27	0.891 (4)	1.896 (4)	1.017 (3)	0.037 (11)*
C28	0.7599 (4)	1.7619 (4)	0.8931 (3)	0.0323 (9)
H28	0.797 (4)	1.683 (4)	0.878 (3)	0.032 (10)*

Atomic displacement parameters (Å²)

	U^{11}	U^{22}	U^{33}	U^{12}	U^{13}	U^{23}
Ni1	0.0255 (3)	0.0314 (3)	0.0272 (3)	0.0115 (2)	0.00572 (19)	0.0066 (2)
S1	0.0248 (5)	0.0345 (5)	0.0274 (5)	0.0125 (4)	0.0033 (4)	0.0058 (4)
S2	0.0244 (5)	0.0326 (6)	0.0318 (5)	0.0091 (4)	0.0050 (4)	0.0065 (4)
S3	0.0240 (5)	0.0328 (5)	0.0282 (5)	0.0098 (4)	0.0041 (4)	0.0054 (4)
S4	0.0239 (5)	0.0308 (5)	0.0308 (5)	0.0102 (4)	0.0063 (4)	0.0071 (4)
F1	0.0403 (12)	0.0353 (13)	0.0334 (12)	0.0142 (10)	−0.0010 (10)	0.0035 (10)
F2	0.0407 (15)	0.0612 (18)	0.144 (3)	0.0355 (14)	0.0282 (16)	0.0254 (18)
F3	0.0303 (12)	0.0822 (19)	0.0542 (15)	0.0280 (12)	0.0184 (11)	0.0323 (14)
F4	0.0683 (17)	0.0385 (15)	0.0509 (16)	0.0048 (13)	−0.0035 (13)	−0.0083 (12)
C1	0.032 (2)	0.037 (2)	0.0262 (19)	0.0194 (18)	0.0090 (16)	0.0125 (17)
C2	0.031 (2)	0.028 (2)	0.029 (2)	0.0132 (17)	0.0121 (16)	0.0135 (17)
C3	0.031 (2)	0.028 (2)	0.030 (2)	0.0171 (16)	0.0059 (16)	0.0114 (17)
C4	0.033 (2)	0.030 (2)	0.028 (2)	0.0157 (17)	0.0091 (16)	0.0120 (17)
C5	0.0238 (18)	0.035 (2)	0.027 (2)	0.0138 (16)	0.0039 (15)	0.0104 (17)
C6	0.029 (2)	0.038 (2)	0.026 (2)	0.0152 (18)	0.0072 (17)	0.0094 (18)
C7	0.027 (2)	0.033 (2)	0.039 (2)	0.0111 (18)	0.0042 (18)	0.0138 (19)
C8	0.034 (2)	0.031 (2)	0.026 (2)	0.0154 (17)	−0.0035 (17)	0.0045 (17)
C9	0.033 (2)	0.037 (2)	0.031 (2)	0.0149 (19)	0.0077 (18)	0.0051 (19)
C10	0.029 (2)	0.038 (2)	0.034 (2)	0.0071 (19)	0.0067 (18)	0.0126 (19)
C11	0.0225 (19)	0.035 (2)	0.031 (2)	0.0097 (16)	0.0007 (16)	0.0067 (17)
C12	0.025 (2)	0.035 (2)	0.045 (2)	0.0079 (18)	0.0046 (18)	0.016 (2)
C13	0.034 (2)	0.033 (3)	0.070 (3)	0.013 (2)	0.000 (2)	0.018 (2)
C14	0.027 (2)	0.045 (3)	0.078 (3)	0.021 (2)	0.006 (2)	0.011 (2)
C15	0.027 (2)	0.053 (3)	0.090 (4)	0.015 (2)	0.025 (2)	0.028 (3)
C16	0.031 (2)	0.033 (2)	0.064 (3)	0.0116 (19)	0.013 (2)	0.019 (2)
C17	0.0242 (19)	0.025 (2)	0.034 (2)	0.0089 (16)	0.0034 (16)	0.0100 (17)
C18	0.027 (2)	0.050 (3)	0.033 (2)	0.0179 (19)	0.0059 (17)	0.0184 (19)
C19	0.034 (2)	0.055 (3)	0.034 (2)	0.022 (2)	0.0109 (18)	0.022 (2)
C20	0.024 (2)	0.045 (3)	0.044 (2)	0.0175 (18)	0.0124 (18)	0.018 (2)
C21	0.022 (2)	0.046 (3)	0.036 (2)	0.0152 (18)	0.0001 (17)	0.0137 (19)

C22	0.032 (2)	0.039 (2)	0.025 (2)	0.0125 (18)	0.0016 (17)	0.0108 (18)
C23	0.0255 (19)	0.034 (2)	0.030 (2)	0.0108 (16)	0.0083 (16)	0.0131 (17)
C24	0.032 (2)	0.036 (2)	0.035 (2)	0.0146 (19)	0.0055 (18)	0.0105 (19)
C25	0.045 (3)	0.034 (3)	0.047 (3)	0.018 (2)	0.013 (2)	0.009 (2)
C26	0.043 (2)	0.036 (2)	0.034 (2)	0.004 (2)	0.004 (2)	0.0021 (19)
C27	0.027 (2)	0.043 (3)	0.040 (3)	0.0033 (19)	−0.0017 (19)	0.012 (2)
C28	0.025 (2)	0.032 (2)	0.038 (2)	0.0091 (18)	0.0068 (17)	0.0107 (19)

Geometric parameters (Å, º)

Ni1—S4	2.1189 (15)	C11—C12	1.388 (5)
Ni1—S1	2.1213 (15)	C12—C13	1.374 (5)
Ni1—S3	2.1217 (11)	C12—H12	0.90 (3)
Ni1—S2	2.1344 (11)	C13—C14	1.372 (6)
S1—C1	1.714 (3)	C13—H13	0.86 (4)
S2—C2	1.705 (4)	C14—C15	1.349 (6)
S3—C3	1.704 (4)	C15—C16	1.382 (6)
S4—C4	1.710 (3)	C15—H15	0.89 (4)
F1—C8	1.372 (4)	C16—H16	0.91 (4)
F2—C14	1.358 (4)	C17—C18	1.390 (5)
F3—C20	1.361 (4)	C17—C22	1.398 (5)
F4—C26	1.369 (4)	C18—C19	1.379 (5)
C1—C2	1.393 (5)	C18—H18	0.92 (3)
C1—C5	1.478 (5)	C19—C20	1.380 (5)
C2—C11	1.487 (5)	C19—H19	1.00 (4)
C3—C4	1.396 (5)	C20—C21	1.362 (5)
C3—C17	1.488 (5)	C21—C22	1.382 (5)
C4—C23	1.470 (5)	C21—H21	0.94 (4)
C5—C6	1.388 (5)	C22—H22	0.99 (4)
C5—C10	1.402 (5)	C23—C28	1.391 (5)
C6—C7	1.383 (5)	C23—C24	1.403 (5)
C6—H6	0.98 (3)	C24—C25	1.386 (6)
C7—C8	1.370 (5)	C24—H24	0.94 (4)
C7—H7	0.92 (4)	C25—C26	1.371 (6)
C8—C9	1.372 (5)	C25—H25	0.92 (4)
C9—C10	1.374 (5)	C26—C27	1.357 (6)
C9—H9	0.91 (4)	C27—C28	1.380 (5)
C10—H10	0.94 (3)	C27—H27	0.87 (4)
C11—C16	1.387 (5)	C28—H28	0.96 (4)
S4—Ni1—S1	176.95 (4)	C14—C13—H13	122 (2)
S4—Ni1—S3	90.79 (5)	C12—C13—H13	121 (2)
S1—Ni1—S3	87.71 (5)	C15—C14—F2	119.2 (4)
S4—Ni1—S2	89.36 (5)	C15—C14—C13	123.0 (4)
S1—Ni1—S2	91.59 (5)	F2—C14—C13	117.8 (4)
S3—Ni1—S2	168.77 (4)	C14—C15—C16	119.2 (4)
C1—S1—Ni1	105.36 (13)	C14—C15—H15	120 (3)
C2—S2—Ni1	104.64 (13)	C16—C15—H15	120 (3)

C3—S3—Ni1	105.74 (13)	C15—C16—C11	119.9 (4)
C4—S4—Ni1	106.05 (14)	C15—C16—H16	120 (2)
C2—C1—C5	124.8 (3)	C11—C16—H16	120 (2)
C2—C1—S1	118.4 (3)	C18—C17—C22	118.3 (3)
C5—C1—S1	116.9 (3)	C18—C17—C3	121.9 (3)
C1—C2—C11	121.9 (3)	C22—C17—C3	119.6 (3)
C1—C2—S2	119.6 (3)	C19—C18—C17	121.2 (4)
C11—C2—S2	118.4 (3)	C19—C18—H18	120 (2)
C4—C3—C17	125.9 (3)	C17—C18—H18	118 (2)
C4—C3—S3	118.8 (3)	C18—C19—C20	118.0 (4)
C17—C3—S3	115.2 (3)	C18—C19—H19	122 (2)
C3—C4—C23	126.6 (3)	C20—C19—H19	119 (2)
C3—C4—S4	118.0 (3)	C21—C20—F3	118.8 (3)
C23—C4—S4	115.3 (3)	C21—C20—C19	123.1 (3)
C6—C5—C10	118.6 (3)	F3—C20—C19	118.1 (3)
C6—C5—C1	120.1 (3)	C20—C21—C22	118.1 (3)
C10—C5—C1	121.2 (3)	C20—C21—H21	124 (2)
C7—C6—C5	121.1 (3)	C22—C21—H21	118 (2)
C7—C6—H6	122 (2)	C21—C22—C17	121.2 (3)
C5—C6—H6	116.9 (19)	C21—C22—H22	116 (2)
C8—C7—C6	118.0 (4)	C17—C22—H22	122 (2)
C8—C7—H7	122 (2)	C28—C23—C24	118.6 (4)
C6—C7—H7	120 (2)	C28—C23—C4	120.3 (3)
F1—C8—C7	118.1 (3)	C24—C23—C4	121.0 (3)
F1—C8—C9	118.8 (3)	C25—C24—C23	120.3 (4)
C7—C8—C9	123.1 (4)	C25—C24—H24	123 (3)
C8—C9—C10	118.5 (4)	C23—C24—H24	117 (3)
C8—C9—H9	125 (2)	C26—C25—C24	118.4 (4)
C10—C9—H9	117 (2)	C26—C25—H25	124 (3)
C9—C10—C5	120.7 (4)	C24—C25—H25	117 (3)
C9—C10—H10	119 (2)	C27—C26—F4	118.3 (4)
C5—C10—H10	120 (2)	C27—C26—C25	123.0 (4)
C16—C11—C12	118.9 (4)	F4—C26—C25	118.6 (4)
C16—C11—C2	121.6 (4)	C26—C27—C28	118.7 (4)
C12—C11—C2	119.5 (3)	C26—C27—H27	120 (3)
C13—C12—C11	121.3 (4)	C28—C27—H27	122 (3)
C13—C12—H12	117 (2)	C27—C28—C23	120.9 (4)
C11—C12—H12	122 (2)	C27—C28—H28	121 (2)
C14—C13—C12	117.6 (4)	C23—C28—H28	118 (2)

Ni1—S1—C1—C2	−1.9 (3)	C11—C12—C13—C14	0.0 (6)
Ni1—S1—C1—C5	177.5 (2)	C12—C13—C14—C15	2.2 (7)
C5—C1—C2—C11	−4.8 (6)	C12—C13—C14—F2	−178.4 (4)
S1—C1—C2—C11	174.6 (3)	F2—C14—C15—C16	178.9 (4)
C5—C1—C2—S2	177.5 (3)	C13—C14—C15—C16	−1.8 (8)
S1—C1—C2—S2	−3.1 (4)	C14—C15—C16—C11	−0.9 (7)
Ni1—S2—C2—C1	6.4 (3)	C12—C11—C16—C15	3.0 (6)
Ni1—S2—C2—C11	−171.4 (3)	C2—C11—C16—C15	−174.5 (4)

Ni1—S3—C3—C4	7.3 (3)	C4—C3—C17—C18	−45.4 (5)
Ni1—S3—C3—C17	−168.9 (2)	S3—C3—C17—C18	130.4 (3)
C17—C3—C4—C23	−8.8 (6)	C4—C3—C17—C22	140.6 (4)
S3—C3—C4—C23	175.5 (3)	S3—C3—C17—C22	−43.6 (4)
C17—C3—C4—S4	173.2 (3)	C22—C17—C18—C19	1.0 (6)
S3—C3—C4—S4	−2.5 (4)	C3—C17—C18—C19	−173.1 (4)
Ni1—S4—C4—C3	−3.7 (3)	C17—C18—C19—C20	−0.9 (6)
Ni1—S4—C4—C23	178.1 (2)	C18—C19—C20—C21	0.3 (6)
C2—C1—C5—C6	136.9 (4)	C18—C19—C20—F3	179.8 (3)
S1—C1—C5—C6	−42.4 (4)	F3—C20—C21—C22	−179.3 (3)
C2—C1—C5—C10	−44.1 (5)	C19—C20—C21—C22	0.3 (6)
S1—C1—C5—C10	136.6 (3)	C20—C21—C22—C17	−0.2 (6)
C10—C5—C6—C7	1.3 (5)	C18—C17—C22—C21	−0.4 (6)
C1—C5—C6—C7	−179.6 (3)	C3—C17—C22—C21	173.8 (3)
C5—C6—C7—C8	1.0 (6)	C3—C4—C23—C28	136.3 (4)
C6—C7—C8—F1	176.8 (3)	S4—C4—C23—C28	−45.6 (4)
C6—C7—C8—C9	−2.2 (6)	C3—C4—C23—C24	−48.0 (5)
F1—C8—C9—C10	−178.0 (3)	S4—C4—C23—C24	130.1 (3)
C7—C8—C9—C10	1.0 (6)	C28—C23—C24—C25	0.7 (6)
C8—C9—C10—C5	1.4 (6)	C4—C23—C24—C25	−175.1 (4)
C6—C5—C10—C9	−2.6 (6)	C23—C24—C25—C26	−1.3 (6)
C1—C5—C10—C9	178.4 (3)	C24—C25—C26—C27	0.6 (7)
C1—C2—C11—C16	125.5 (4)	C24—C25—C26—F4	−178.8 (4)
S2—C2—C11—C16	−56.8 (5)	F4—C26—C27—C28	−180.0 (3)
C1—C2—C11—C12	−51.9 (5)	C25—C26—C27—C28	0.6 (7)
S2—C2—C11—C12	125.8 (3)	C26—C27—C28—C23	−1.2 (6)
C16—C11—C12—C13	−2.6 (6)	C24—C23—C28—C27	0.6 (6)
C2—C11—C12—C13	174.9 (4)	C4—C23—C28—C27	176.4 (3)

Hydrogen-bond geometry (Å, º)

D—H···*A*	*D*—H	H···*A*	*D*···*A*	*D*—H···*A*
C19—H19···F1^{i}	1.00 (4)	2.47 (4)	3.136 (5)	123 (3)

Symmetry code: (i) *x*, *y*+1, *z*+1.